A test for rate-coupling of trophic and cranial evolutionary dynamics in New World bats

Jeff J. Shi,[1,2,3,4] (iD) **Erin P. Westeen,**[2,5,6] (iD) **and Daniel L. Rabosky**[2,3] (iD)

[1]*Minnesota Supercomputing Institute, University of Minnesota, Minneapolis, Minnesota 55455*

[2]*Museum of Zoology, University of Michigan, Ann Arbor, Michigan 48109*

[3]*Department of Ecology and Evolutionary Biology, University of Michigan, Ann Arbor, Michigan 48109*

 [4]*E-mail: jeffjshi@umich.edu*

[5]*Museum of Vertebrate Zoology, University of California Berkeley, Berkeley, California 94720*

[6]*Department of Environmental Science, Policy, and Management, University of California Berkeley, Berkeley, California 94720*

**Morphological evolution is often assumed to be causally related to underlying patterns of ecological trait evolution. However, few studies have directly tested whether evolutionary dynamics of—and major shifts in—ecological resource use are coupled with morphological shifts that may facilitate trophic innovation. Using diet and multivariate cranial (microCT) data, we tested whether rates of trophic and cranial evolution are coupled in the radiation of New World bats. We developed a generalizable information-theoretic method for describing evolutionary rate heterogeneity across large candidate sets of multirate evolutionary models, without relying on a single best-fitting model. We found considerable variation in trophic evolutionary dynamics, in sharp contrast to a largely homogeneous cranial evolutionary process. This dichotomy is surprising given established functional associations between overall skull morphology and trophic ecology. We suggest that assigning discrete trophic states may underestimate trophic generalism and opportunism, and that this radiation could be characterized by labile crania and a homogeneous dynamic of generally high morphological rates. Overall, we discuss how trophic classifications could substantively impact our interpretation of how these dynamics covary in adaptive radiations.**

KEY WORDS: Chiroptera, ecological evolution, microCT, shape evolution, trophic evolution.

Ecological diversity and morphological disparity are closely linked throughout biology and the tree of life. For example, phenotypic traits are tied to mechanical performance (Arnold 1983; Kingsolver and Huey 2003), which governs aspects of organismal ecology like locomotion and the processing of food (Losos 1990; Berwaerts et al. 2002; Calsbeek and Irschick 2007). Many studies have documented relationships between morphology and ecology ("ecomorphology"), to the extent that quantitative measurements of morphological traits are frequently used as proxies for ecology (Miles and Ricklefs 1984; Dawideit et al. 2009; Zanno and Makovicky 2011).

The prevalence of ecomorphological associations may lead us to assume that evolutionary dynamics of ecology and morphology are typically coupled. Adaptive radiations, for example, are characterized by shifts to rapid ecological and morphological evolution during the diversification process (Stebbins 1970; Sturmbauer 1998; Schluter 2000; Losos and Mahler 2010). Ecological opportunity can promote speciation by driving adaptation and reinforcing isolation among lineages (Schluter 1996; Rundell and Price 2009). Morphological divergence further facilitates this process, leading to a prediction that rates of diversification, ecological innovation, and disparification
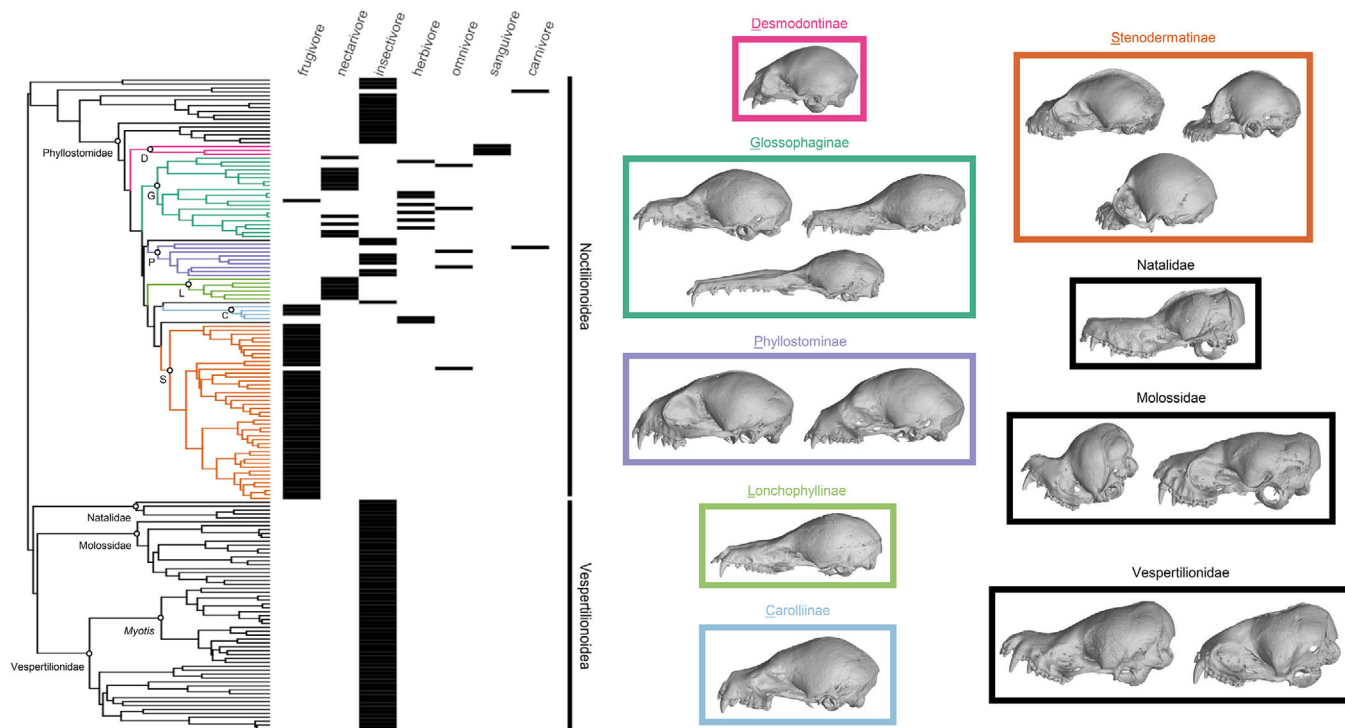
Figure 1. Phylogeny of New World bats and representative crania. The full species-level phylogeny of New World bats included in this study (Shi and Rabosky 2015). On the phylogeny, various major clades referred to within the text are labeled; some subfamilies of the family Phyllostomidae are both colored and lettered. Adjacent to this phylogeny, the black barcodes indicate trophic guild classification used for this study. On the right side, representative crania (not to scale) illustrate the diversity of cranial morphologies across the clade. In order from left to right, top to bottom, the depicted species are as follows: *Diaemus youngi, Glossophaga leachii, Hylonycteris underwoodi, Musonycteris harrisoni, Chiroderma trinitatum, Phylloderma stenops, Lonchophylla mordax, Carollia subrufa, Artibeus jamaicensis, Ametrida centurio, Sphaeronycteris toxophyllum, Nyctiellus lepidus, Mormoops megalophylla, Tadarida brasiliensis, Myotis volans*, and *Lasiurus cinereus*. Colors for polygons and text and underlined letter abbreviations match those of the phyllostomid subfamilies on the tree.

all covary during an adaptive radiation—and furthermore, that shifts in rates of these evolutionary dimensions typically occur in concert. Numerous clades are characterized by rate-coupling of evolutionary dynamics (e.g., Gillespie 2004; Cozzolino and Widmer 2005; Wagner et al. 2012). Although many studies test whether dynamics of speciation and morphological evolution covary across radiations (Gould and Eldredge 1993; Yang 2001; Ricklefs 2004; Rabosky et al. 2013; Cooney and Thomas 2020), fewer studies test explicitly for rate-coupling of ecology and morphology, especially with regard to the timing and location of major shifts in the tempo of these two evolutionary dimensions.

Bats are widely considered a large-scale adaptive radiation (cf. Osborn 1902; Simpson 1953). The clade (Order Chiroptera) is characterized by variation in species richness, ecology, and morphology across its subclades (Simmons and Conway 2003; Jones et al. 2005). For example, the largest bat superfamily Vespertilionoidea mostly comprises obligate insectivores like the cosmopolitan genus *Myotis* (subfamily Myotinae, Fig. 1; Nowak 1994; Simmons 2005). The predominantly Neotropical

superfamily Noctilionoidea, by contrast, is characterized by high trophic diversity (Dumont et al. 2012). These two superfamilies diverged relatively early in the history of crown Chiroptera (~55 million years ago; Shi and Rabosky 2015), and encompass most of extant, global bat species richness. Previous researchers have inferred coupled and fast rates of morphological evolution and speciation among noctilionoids (Monteiro and Nogueira 2011; Dumont et al. 2012; Rojas et al. 2018). In many species, skull morphology, performance, and trophic behavior are biomechanically predictive of each other (Dumont et al. 2009; Santana and Dumont 2009). Bat skull shapes clearly dictate bite force and abilities to process different materials (Santana et al. 2010; Santana et al. 2012). However, it is unclear whether shape lability is dynamically linked with the lability of discrete ecological traits like trophic behavior, which may underlie overall innovation and adaptation. Skull morphology may also be more loosely connected to general ecology than to more specific measures of biomechanical performance like bite force. Furthermore, bat skulls may be highly modular, with potentially large differences

between the cranium and mandible in terms of functional ecology. It is thus unclear if rate shifts of trophic and morphological evolution would be coupled at evolutionary timescales for a particular module of the bat skull, such as the cranium.

Here, we test for rate-coupling between the dynamics of trophic and cranial evolution in these two superfamilies, across the New World. In the Nearctic, nearly all ∼40 extant species are insectivorous vespertilionoids like *Myotis* (Fig. 1; Nowak 1994; Simmons 2005). By contrast, noctilionoids (>250 species) are among the most speciose clades of mammals in the Neotropics (Fleming and Kress 2013), and include many frugivores, nectarivores, and omnivores (Simmons 2005; Monteiro and Nogueira 2011; Dumont et al. 2012). The most diverse noctilionoid clade is the family Phyllostomidae, with a subfamily taxonomy that historically reflects observed ecological and morphological diversity (Fig. 1). One possible explanation for these contrasting patterns of clade diversity is that rate transitions and dynamics of trophic, morphological, and species diversification are all coupled: subclades with low richness and trophic diversity (e.g., Nearctic vespertilionids) are characterized by shifts to low rates of diversification and morphological evolution, corresponding to low rates of innovation in trophic niche space. By contrast, we would expect to find shifts to rapid evolutionary rates for both trophic state and morphology among the trophically diverse Neotropical noctilionoids, especially in rapidly diversifying clades. We may thus expect to find an overall rate-coupling of both trophic innovation and morphological evolution. Here, we quantify these two evolutionary dynamics using diet data and a high-dimensional morphological dataset of bat crania, and test the extent to which they covary across the radiation.

Materials and Methods
PHYLOGENY AND TROPHIC STATE
We used the phylogeny of Shi and Rabosky (2015), as updated by Shi et al. (2018a), for this study. We classified all species by biogeographic realm (Olson et al. 2001), superfamily, family, and subfamily, as described by Simmons (2005), Teeling et al. (2005), and Rojas et al. (2016).

We then assigned each species to a trophic guild using diet data. These data were initially compiled from a literature review and field observations, and were published as diet data and guild classifications by Rojas et al. (2016, 2018). We followed these studies and used their 60% dietary cutoff for assigning a single, specialist guild—for example, if a bat's diet is more than 60% insects by composition, this species would be classified as a specialist insectivore (Table S1). Following Rojas et al.'s framework, we classified bats that consume both animals and plants as omnivores, and bats that consume both nectar and fruit as herbivores. Importantly, we note that although these authors prioritized quan-

titative, field data whenever possible, knowledge of some diets is fragmentary and restricted to literature review. We used these trophic guild classifications as character states for our subsequent analyses. The overall phylogenetic framework of our study is depicted in Fig. 1 (see also Fig. S9).

TROPHIC EVOLUTION
To infer dynamics of trophic evolution, we fitted a set of phenotypic evolutionary models that allowed rates of character state evolution to vary in partitions across the phylogeny (sensu Davis Rabosky et al. 2016). In these models, rate matrices describe transition rates among different trophic states. We constructed these partitioned models using the R package *diversitree* (FitzJohn 2012). However, because the package currently has no implementation of partitioned, character-independent (split-Mk) models, we implemented them by constraining split-MuSSE (partitioned/split, multistate, speciation, and extinction) models to have equal diversification rates across character states. Note that the relative likelihood of the data with respect to our *character rates* of interest is mathematically independent of the diversification rates when constrained in this way. Due to potential nonidentifiability concerns associated with asymmetric transition rates (Grundler and Rabosky 2020b), we only considered symmetric transition rates in each partition (i.e., combinations of Mk1 processes).

Our trophic analyses comprised three classes of models: (1) a *one*-partition model with only a single, global rate across the phylogeny, thus modeling evolutionary rates with a single, global rate matrix defining transitions among trophic states; (2) all possible *two*-partition (two-rate) models where partition location was constrained to the set of all internal nodes (i.e., a phylogeny with k tips has $k - 1$ possible partitions and rate matrices), and (3) all possible *three*-partition models for our dataset defined by identifying all unique node *pairs*, each pair partitioning the phylogeny into three groups. Note that, in each case, we assume that trophic switching rates may differ between partitions, but that all transitions within a partition are governed by a single rate parameter. A two-partition model, for example, can be viewed as a scenario where one lineage and all its descendants undergo a regime shift in trophic evolutionary dynamics, such that rates of transition among trophic states change (and thus, evolve under a different rate matrix relative to the ancestor). For all partitioned models, we set equal transition rates $q_{i,j}$ among trophic states *within* partitions (i.e., a single transition rate is estimated for each partition), but allowed these rates to vary *across* partitions. We maximized the log-likelihood of the data under all possible one-, two-, and three-partition split-Mk models across the phylogeny. It was computationally impractical to add additional partitions for this study, as even adding a fourth partition increases the overall

sample space by over fiftyfold relative to the three-partition case (>735,000 additional models).

Our analyses considered 13,696 total models. Due to the potential for many models to have similar explanatory power, we used model-averaging within an information-theoretic framework of parameter estimation that considered the relative performance of *all* models in the candidate set. To characterize overall rate heterogeneity across the tree, we estimated macroevolutionary "cohorts," where a cohort is a set of taxa that are inferred to have evolved under a shared, inherited evolutionary rate regime (Rabosky et al. 2014a; Fig. S1). Operationally, we defined a metric for cohort pairwise probability as the probability that two taxa belong to the same evolutionary rate regime/cohort, summed across all models in the candidate set, and weighted by the relative probability of each split-Mk model.

Pairwise cohort probability $P_{i,j}$ is thus the probability that the i-th and j-th species share a common evolutionary rate regime. Because rate regimes are unique (i.e., the regime states are nonrecurrent), the assignment of two species to the same rate regime or cohort implies that they share evolutionary rate parameters due to common ancestry. Evolutionary rate regimes can represent paraphyletic character states if additional, nested subclades undergo a secondary rate shift. Accommodating and visualizing such paraphyly was a primary motivation for the development of cohort-based frameworks (Rabosky et al. 2014a). Let $W_{z,k}$ denote the Akaike weight of a submodel (z, k), defined by the k-th unique partition of a model class with z partitions ($z \in \{1, 2, 3\}$). We then estimate the pairwise cohort probability as

$$P_{i,j} = \sum_{z=1}^{3} \sum_{k=1}^{S(z)} W_{z,k} I_{i,j,z,k,}$$

where $S(z)$ is the total number of unique partition configurations for the set of submodels with z partitions (e.g., $S(z) = 13{,}530$ for $z = 3$). $I_{i,j,z,k}$ is an indicator variable that takes a value of 1 if the i-th and j-th species were assigned the same evolutionary rate class for submodel (z, k), and 0 otherwise. Hence, values approach $P_{i,j} = 1$ when the i-th and j-th species share an identical rate regime across the set of most-probable submodels. Note that all species are assigned to the same rate regime when $z = 1$ (one partition). As such, if this model has a much higher weight than all others in the candidate set, all species would necessarily have weighted cohort probabilities approaching 1. Statistical properties of cohort matrices and their utility for understanding complex macroevolutionary dynamics are provided in Rabosky et al. (2014a).

In addition to assigning species to cohorts, we estimated branch-specific transition rates using an analogous model-averaging approach. We first note that each submodel (z, k) defines a mapped set of evolutionary rates across the phylogeny,

such that each branch in the phylogeny is assigned to one of the z rate classes under that submodel. Let $q_{z,k,b}$ denote the evolutionary rate for the b-th branch under submodel (z, k). The weighted rate across all models is thus

$$q_b = \sum_{z=1}^{3} \sum_{k=1}^{S(z)} W_{z,k} q_{z,k,b.}$$

Weighted cohort probabilities and branch rates computed in this fashion incorporate information from the complete set of candidate models, and avoid several pitfalls associated with focusing exclusively on a best-fit model. These approaches also capture additional heterogeneity in processes that cannot adequately be described by the maximum complexity model under consideration (Rabosky et al. 2014a). We used weighted character transition rates, as computed above, to visualize trophic evolution along branches (as transition rates among states) by modifying functions of the *BAMMtools* R package (Rabosky et al. 2014b). We interpret within-partition transition rates as measures of trophic lability that underlie trait evolution. *A posteriori*, we identified well-supported trophic cohorts for downstream analyses of shape evolution, to test if trophic evolution is coupled with cranial shape evolution.

SPECIMENS AND SHAPE QUANTIFICATION

For our morphological analyses, we collected cranial shape data from 167 New World bat specimens within the University of Michigan Museum of Zoology and the American Museum of Natural History. This represents roughly 60% of the estimated extant species diversity across these biogeographic realms. We digitized each cranium using X-ray computed microtomography (μCT) scanning. These data are accessible through a publicly available repository and resource for research (Shi et al. 2018b); for this study, we also incorporated a small ($n = 30$) set of landmarks previously published alongside that repository.

For each cranium, we quantified shape using three-dimensional landmark-based geometric morphometrics. Our landmark set was adapted from a prior analysis intended to broadly quantify shape in bat crania and test hypotheses of modularity; we used this set to encapsulate as much cranial shape diversity as possible. We performed all landmarking in the program Checkpoint (Stratovan, Davis, USA). Each cranium was represented by a set of 18 unique, homologous landmarks. As 11 of these are symmetrical points, we digitized a total of 29 fixed landmarks per cranium. We additionally generated 15 equidistant semilandmarks along the midline of the cranium (Fig. S2). This set of 44 total points was specifically adapted from Santana and Lofgren (2013).

After landmarking each specimen and generating a species-level dataset of three-dimensional coordinates, we performed most subsequent shape analyses using the R package *geomorph*

version 3.0.6 (Adams et al. 2017). We first estimated the coordinates of any missing landmarks (e.g., on damaged crania) by aligning incomplete specimens to complete specimens, and using a thin-plate spline to estimate missing data (Gunz et al. 2009).

We transformed these raw coordinate data using a generalized Procrustes analysis that aligned the dataset within a common coordinate system, scaled by centroid size (Rohlf and Slice 1990). During this alignment, we allowed semilandmarks to slide along curves using the Procrustes distance criterion (Rohlf 2010). The resulting superimposed coordinates served as shape variables for each specimen. During superimposition, we also calculated centroid size, which are often used as a proxy for overall size (Kosnik et al. 2006; McGuire 2010; Zelditch et al. 2017).

CRANIAL SHAPE VARIATION

We assessed phylogenetic signal of cranial shape using the multivariate K statistic (K_{mult}) (Blomberg et al. 2003; Adams 2014a). We then tested for any relationships between shape disparity and clade membership, trophic guild, or trophic cohort membership by using phylogenetic generalized least squares (PGLS; Adams 2014b; Adams and Collyer 2015). We also tested for these relationships using multivariate generalized least squares (mvGLS) to account for potentially elevated Type 1 error rates in the multivariate implementation of PGLS (Clavel and Morlon 2020). To correct for phylogenetic nonindependence of data, we followed Serb et al. (2017) and calculated phylogenetic disparity using *geomorph*, assessing significance using 1000 permutations of the observed data.

To reduce the dimensionality of the dataset for some subsequent analyses, we ordinated our data using a principal component (PC) analysis. As with the multivariate data, we calculated the K statistic to test for phylogenetic signal (Blomberg et al. 2003). We also tested for and removed potential effects of allometry from the PC data, as in other shape studies (Sherratt et al. 2014; Santana and Cheung 2016). We first confirmed significant allometric effects using a PGLS of shape on centroid size. We then added the residuals from this PGLS to the phylogenetic mean of the aligned coordinates, and performed a PC analysis on these transformed data (Klingenberg and Marugán-Lobón 2013; Sherratt et al. 2014). We used these allometry-free PC scores for some downstream analyses. However, we emphasize that the original PC scores and these allometry-free scores are well-correlated ($P < 0.001$, mean $r = 0.78$), especially among the first three PC axes (mean $r = 0.94$).

CRANIAL SHAPE EVOLUTION

We calculated multivariate rates of shape evolution using two different modes of methods (*sensu* Adams 2014c). The first, termed an **R**-mode method, used phylogenetic variance-covariance matrices, where diagonals represent rates (σ^2), and off-diagonals represent covariances among traits (Revell and Harmon 2008; Revell and Collar 2009; Adams 2014c). There are two important caveats of **R**-mode methods. First, data matrices where the dimensionality of the traits equals or exceeds the number of taxa are singular, rendering likelihood calculations impossible. However, accounting for this by reducing dimensionality (e.g., using a subset of PC axes) can unfortunately inflate Type 1 error rates if one is also selecting and fitting non-Brownian motion (BM) models of trait evolution (Adams 2014c; Adams and Collyer 2018). Because we necessarily needed to reduce the dimensionality of the dataset (i.e., our traits exceeded our number of species), we thus also restricted these **R**-mode analyses to BM models of trait evolution (see Supporting Information for initial tests of Ornstein-Uhlenbeck models).

We performed these **R**-mode multivariate analyses using the R package *mvMORPH* (Clavel et al. 2015). Specifically, we fitted single-rate and multirate BM models of shape evolution to the first three PC axes, which explained 64% of the total shape variance. *mvMORPH* allows for model selection of constraints to BM rate matrices in **R**-mode morphological analyses (Table S3). Each of these potentially constrained rate matrices represents different scenarios for whether traits evolve independently across and/or within partitions; however, it was computationally infeasible to fit every potential suite of constraints to the full set of partition configurations. To select one of these constraints, we held partition configuration constant for an initial pilot model. In this pilot, we used a nested, multirate BM model with different rates assigned to each of the three partitions of the ML split-Mk model of trophic evolution. We then selected the best-fitting BM rate matrix model from this pilot test for the subsequent **R**-mode analyses.

To conceptually echo the split-Mk analyses of trophic evolution, we adapted a similar partitioned framework and cohort inference approach. We first fit a single-rate (termed BM1 in *mvMORPH*) model to the entire tree. Then, we fit two-rate and three-rate (multirate BM: termed BMM in *mvMORPH*) models to every node, and to every unique pair of nodes, respectively. In these BMM models, each partition of the phylogeny was characterized by a shift to its own evolutionary rate matrix (sensu Revell and Harmon 2008; Revell and Collar 2009). Note that in this **R**-mode analysis of three PC axes, we could not allow partitions with fewer than four taxa. For each fit, we calculated the model likelihood and inferred rate matrices for all partitions. We then identified candidate cranial shape cohorts by using Akaike weights for each BM model, as in the split-Mk models. We first multiplied each evolutionary rate matrix by the Akaike weight of its generating BM model. We then used the summed diagonals of each partition's matrix as its rate, and visualized rates (σ^2) of shape evolution on the phylogeny using BAMMtools (Rabosky et al. 2014b).

Our second approach for calculating rates of shape evolution is termed a **Q**-mode method and implemented in *geomorph* (Adams 2014c); this method does not require a reduction in dimensionality. These rates (σ^2_{mult}) are net estimates of rates for *a priori* defined groups, under a BM model of trait evolution, calculated using a centered distance matrix between shapes (Adams 2014c; Adams and Collyer 2018). With this method, we were able to calculate σ^2_{mult} as a rate estimate for the *entire* cranium, as opposed to a subset of PC axes. We assessed statistical significance using both simulations and permutations of the observed data (Denton and Adams 2015; Adams and Collyer 2018). We calculated σ^2_{mult} for all families and subfamilies of New World bats, and for both trophic and **R**-mode morphological cohorts, to assess how well trophic evolution is coupled with shape evolution.

Results

SPECIES CHARACTERISTICS

We collected and report geometric shape and trophic data for 167 species of extant New World bats (Table S1). This comprises about 75% (31 species) of estimated Nearctic diversity, and 60% (144 species) of estimated Neotropical diversity, with eight species present in both realms (Fig. 1; Simmons 2005; Shi et al. 2018a). Among noctilionoids, 54% include more than a single type of food in their diet (Table S1). However, using the conservative 60% threshold of Rojas et al. (2018), most noctilionoids are classified as specialists of a single diet category, with only 13% of species classified as omnivores or herbivores (Fig. 1).

TROPHIC EVOLUTION

Out of 13,696 possible one-, two-, and three-partition split-Mk models, where each species is assigned a discrete trophic guild state (sensu Rojas et al. 2018), only 14 individually contribute more than 1% to the total Akaike weight. These 14 models accounted for 54.5% of the probability of the data given the full candidate set of models, with the overall best model accounting for 26.2% of the total Akaike weight (Fig. S3). This model with the highest Akaike weight is a model with three partitions: a paraphyletic background regime, a regime shift for a paraphyletic partition including most phyllostomids, and a regime shift comprising a monophyletic partition for the phyllostomid subfamily Stenodermatinae. However, the model with the next-highest Akaike weight (Δ weight = 0.224) only differs by the inclusion of a single branch (*Rhinophylla*) into the stenodermatine clade.

Not needing to rely on a single "best" model, and the presence of many models with similar and/or weak explanatory power, highlights a strength of model-averaged analyses. Cohort analyses like ours summarize broad patterns of shared evolu-

tionary rate dynamics across taxa, and allow general patterns to emerge even when many models have equivocal and/or poor support. We use this approach to identify candidate trophic cohorts (Fig. 2a). All vespertilionoids (Fig. 1) belong to an independent trophic cohort (median pairwise probability *mpp* = 99%). The other major clades of insectivores, however, including the earliest diverging noctilionoid families and phyllostomid subfamilies, have lower probabilities of belonging to this cohort (*mpp* = 70–90%). Using a conservative threshold of 95% *mpp*, we identify three candidate insectivorous cohorts, all characterized by the *slowest* weighted transition rates across the phylogeny (Fig. 2b; Table 1).

Phyllostomid bats are characterized by substantial heterogeneity in the rate of trophic evolution (Fig. 2a), and we find evidence for five distinct phyllostomid trophic cohorts. Of these cohorts, the predominantly frugivorous subfamily Stenodermatinae is characterized by a shift to relatively slow transition rates (Fig. 2b; Table 1). This contrasts with regimes characterized by rapid rates for a paraphyletic group with many trophic guilds (which we term the "Lonchophyllinae cohort" for brevity), and for a cohort of the predominantly nectarivorous subfamily Glossophaginae.

SHAPE VARIATION AND PATTERNS

We find significant phylogenetic signal in cranial shape among New World bats ($K_{mult} = 0.581$, $P < 0.01$), but few significant predictors of shape among phylogeny, trophic state, or trophic cohort membership using PGLS, and no significant predictors among these categories using mvGLS (Table S2). Although the three major dietary categories—frugivores, insectivores, and nectarivores—are generally separated in trophic diet space, there are many overlapping groups of species, especially among frugivores and insectivores (Fig. 3A). There is even more overlap of our previously identified trophic cohorts within cranial morphospace (Figs. 3B and S9). The first 20 PC axes explain 95% of the variance in the shape data; however, after the first three axes, each subsequent axis only explains 5% or less of the total variance. We find significant phylogenetic signal ($P \leq 0.001$) of scores for all three of these axes: $K = 0.86$, 2.19, and 0.52, respectively. PC1 is most aligned with the length of the snout, and differences along this axis distinguish the subfamily Stenodermatinae from the rest of the clade. As such, it appears to readily discriminate between frugivorous and nectarivorous bats, among the non-insectivores. By contrast, PC2 is associated with snout width and slope, and appears to discriminate between noctilionoids and vespertilionoids—or, in trophic terms, between non-insectivores and insectivores. PC3 is instead associated with the relative height of the cranial vault (see Fig. S6 for more details).
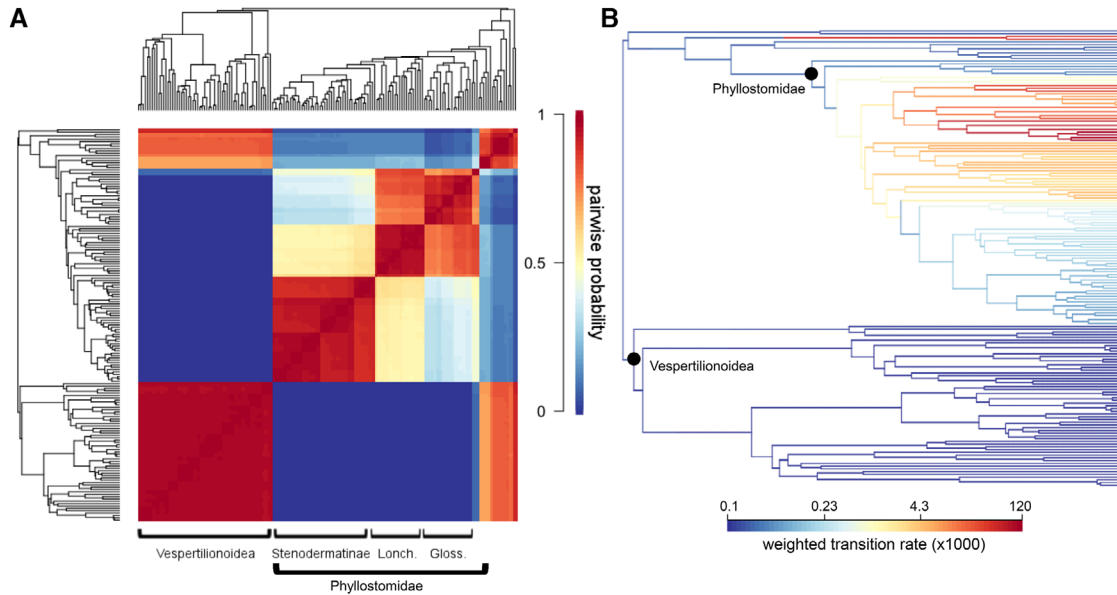
Figure 2. Macroevolutionary dynamics of trophic evolution. (A) Trophic cohorts as inferred by our models of character evolution. The phylogeny is projected on the left and right sides of the matrix. Colors represent weighted pairwise probabilities of belonging to the same partition across all models. See Table 1 for cohort details. (B) Rates of trophic niche evolution, estimated from model-averaged transition rates among ecological states on the bat phylogeny. Two major subclades, Vespertilionoidea and Phyllostomidae, comprise the majority of New World species richness and show dramatic differences in overall evolutionary dynamics. Note that the nonlinear color scheme, which emphasizes heterogeneity within the phyllostomids, also has the side effect of making the subfamily Stenodermatinae and the entire superfamily Vespertilionoidea appear similar (cool colors). However, rates within stenodermatines are more than 20× faster than within vespertilionoids.

Table 1. Trophic cohorts.

Cohort name	Cohort members	Trophic guilds	Median pairwise membership	Median cohort $q_{i,j}$ ($\times 1000$)
Stenodermatinae	Phyllostomidae: subfamily Stenodermatinae	Primarily frugivores	95%	2.31
Lonchophyllinae (Lonch.)	Phyllostomidae: subfamilies Lonchophyllinae, Carolliinae, Glyphonycterinae, Lonchorhininae, Rhinophyllinae, Phyllostominae	Insectivores, carnivores, frugivores, nectarivores, omnivores	98%	4.33
Glossophaginae (Gloss.)	Phyllostomidae: subfamily Glossophaginae	Primarily nectarivores	95%	6.27
Desmodontinae	Phyllostomidae: subfamily Desmodontinae	All obligate sanguivores	100%	3.92
Micronycterinae	Phyllostomidae: subfamilies Micronycterinae, Macrotinae	Primarily insectivores	100%	0.60
Mormoopidae	Mormoopidae, Emballonuridae, Noctilionidae	Primarily insectivores, one piscivore	96%	0.32
Vespertilionoidea	Vespertilionidae, Molossidae, Natalidae	All obligate insectivores in this dataset	99%	0.10

Cohorts identified by our partitioned analyses of trophic evolution. Cohorts are identified without regard to taxonomy, but well-supported cohorts typically correspond to known taxonomic groups, and are named as such. The median pairwise membership of taxa in each cohort is calculated from Akaike weights of all models where cohort members are in the same partition. Each cohort's median character transition rate $q_{i,j}$ is multiplied by 1000 for relative comparison.
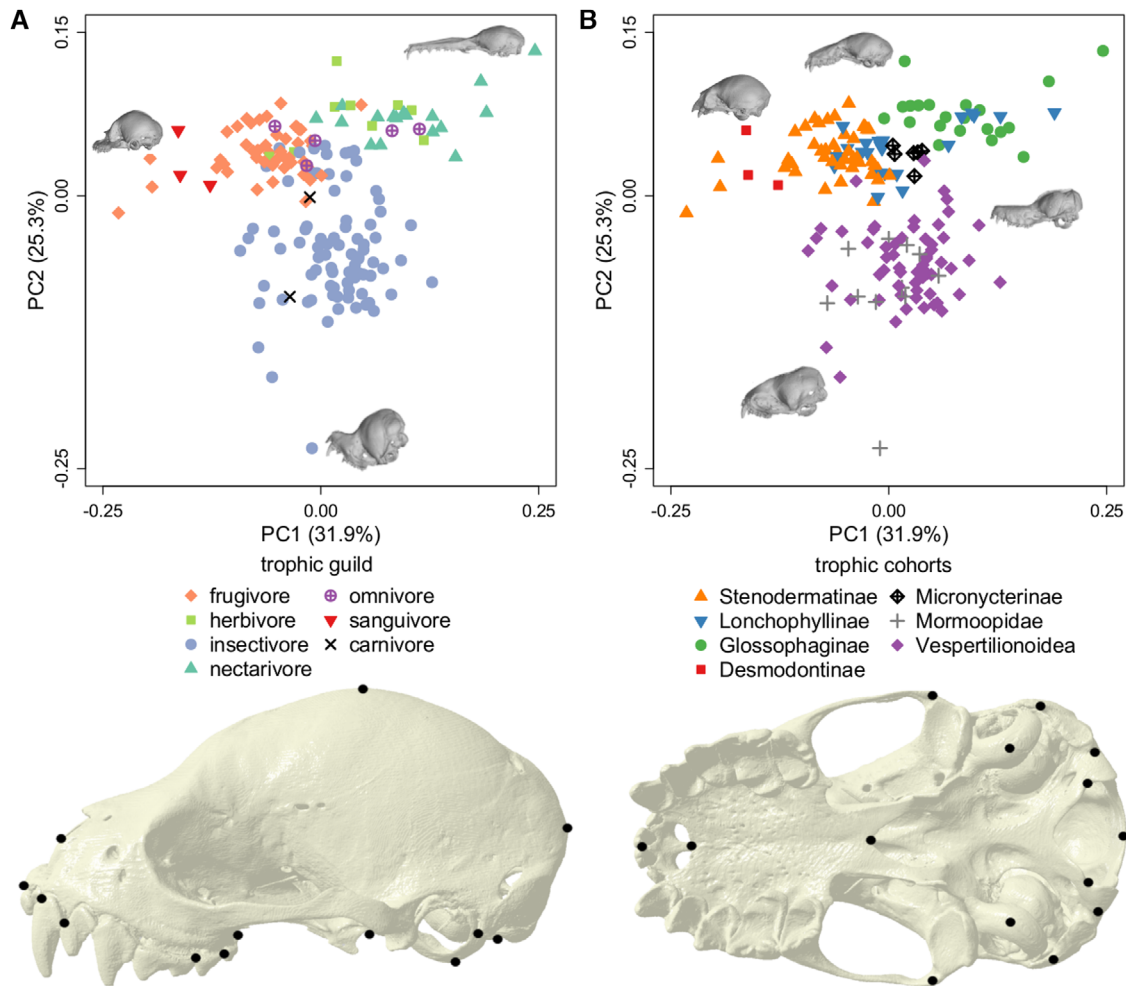
Figure 3. Morphospace of New World bat crania. (A) The first two principal component axes for cranial shape data, highlighting trophic guilds used for our analyses. Inset crania, clockwise from the top: *Musonycteris harrisoni, Mormoops megalophylla, Ametrida centurio*. (B) The same morphological dataset, colored by trophic cohorts (Table 1; note that cohorts we identified are often congruent with named higher taxa and are labeled as such). Inset crania, clockwise from the top: *Erophylla sezekorni, Nyctiellus lepidus, Lasiurus cinereus, Diaemus youngi*. "Other families" comprises Emballonuridae and the smaller, nonphyllostomid noctilionoid families Noctilionidae and Mormoopidae. Below both plots, a sample cranium of *Artibeus aztecus* (Noctilionoidea: Phyllostomidae: Stenodermatinae), with our landmark scheme highlighted on lateral and ventral views. See Supporting Information for expanded landmark details and a higher resolution version. Crania are not to scale.
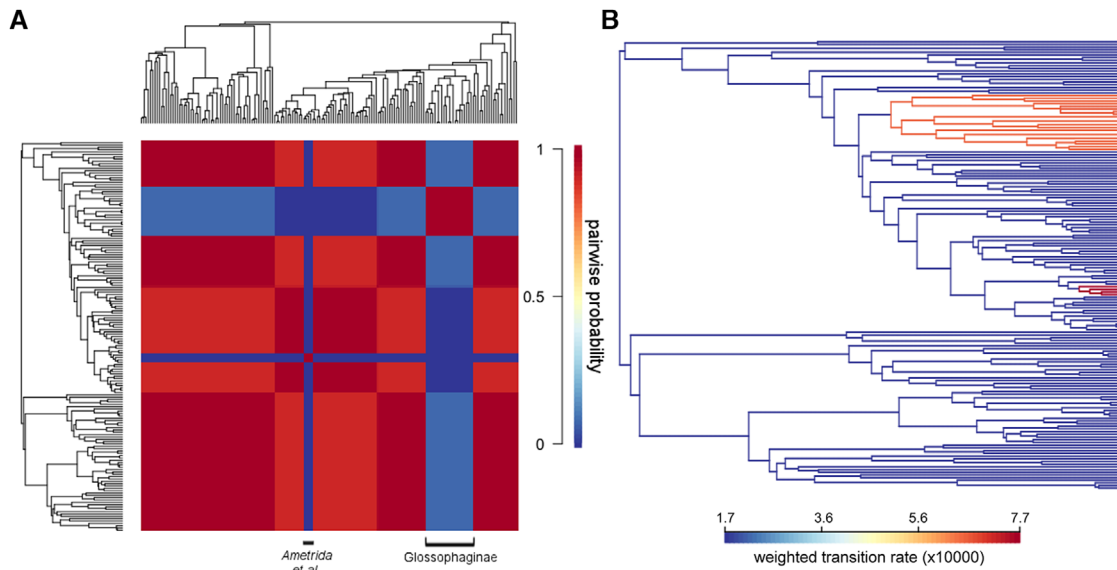
CRANIAL SHAPE EVOLUTION

For **R**-mode analyses, our pilot three-rate BMM model (with the three partitions of the ML split-Mk trophic model) was best supported by unconstrained rate matrices—as such, we selected unconstrained BM1/BMM models for all subsequent **R**-mode analyses (see Table S3 for further discussion). We fit a total of 2,391 single-rate BM1 or two/three-rate BMM models to the shape data (after constraining the set space to partitions with more than four species; Fig. S5). The ML model of shape evolution accounts for 91.6% of the total weight across all models; the statistical dominance of a single model contrasts with our results for diet evolution, where support is more dispersed. This ML BMM model is one with three separate rate matrices: the paraphyletic

background process, and regime shifts for the subfamily Glossophaginae and a small clade of four frugivores in the subfamily Stenodermatinae (*Ametrida* and three allies, *Pygoderma*, *Sphaeronycteris*, and *Centurio*).

In contrast with trophic evolution, we find evidence for fewer well-supported morphological cohorts after weighting all possible models (Fig. 4a). Most New World bats are clearly united into one paraphyletic morphological cohort spanning all trophic states, and the overall pattern after model averaging still reflects a strong signal from the ML model. We summarize these cohort inferences in Table 1. Furthermore, we infer generally homogeneous rates (σ^2) of trait evolution among New World bats with our **R**-mode analyses (Fig. 4), with two exceptions: the

Figure 4. Macroevolutionary dynamics of cranial shape evolution. (A) Morphological cohorts as inferred by multirate BMM models of multivariate trait evolution, using PC axes 1–3. The phylogeny is projected on the left and right sides of the matrix. Colors represent weighted pairwise probabilities of belonging to the same partition across all models. See Table 1 for cohort details. (B) Weighted rates of cranial shape evolution, from the evolutionary rate matrices of multirate BMM models.

Table 2. Morphological shape cohorts.

Cohort name	Cohort members	Trophic guilds	Median pairwise membership	Median cohort σ^2 ($\times 10^4$)	Cohort σ^2_{mult} ($\times 10^5$)
Ametrida complex	Phyllostomidae: subfamily Stenodermatinae: *Ametrida*, *Centurio*, *Pygoderma*, *Sphaeronycteris*	All obligate frugivores	100%	7.67	2.70
Glossophaginae	Phyllostomidae: subfamily Glossophaginae	Primarily nectarivores	100%	6.63	0.78
Background radiation	All other bats	All New World trophic guilds	91.8%	1.74	0.44

Morphological cohorts identified by multirate BM (BMM) analyses on PC1-3. Interpretation is analogous to that of Table 1. σ^2 was calculated from diagonals of evolutionary rate matrices across R-mode models. σ^2_{mult} refers to clade multivariate shape evolution rates calculated under Q-mode analyses; these differ based on both permutations ($P = 0.021$) and simulations ($P < 0.01$).

Glossophaginae and *Ametrida* (and allies) cohorts, which both have elevated rates.

With the **Q**-mode analyses of rates (σ^2_{mult}) of overall cranial shape evolution, we find no significant differences among *a priori* defined taxonomic families, subfamilies, trophic cohorts, or guilds. We do find, however, that the three morphological cohorts defined by *mvMORPH* analyses differ significantly in σ^2_{mult}, with faster rates of shape evolution among Glossophaginae and the complex of *Ametrida* and allies (Table 2). We stress that these overall homogeneous dynamics do not imply morpho-

logical stasis across the clade, however, especially in light of the substantial intraguild disparity visible in PC space (Fig. 3) and across the phylogeny (Fig. S6).

ECOMORPHOLOGICAL DYNAMICS

At the species level, there is a positive linear relationship (OLS $R^2 = 0.286$; Fig. 5) between both model-averaged rates of trophic evolution (split-Mk analyses) and rates of cranial shape evolution (**R**-mode analyses). We do not present a *p*-value for this result, because it appears driven entirely by a single clade of
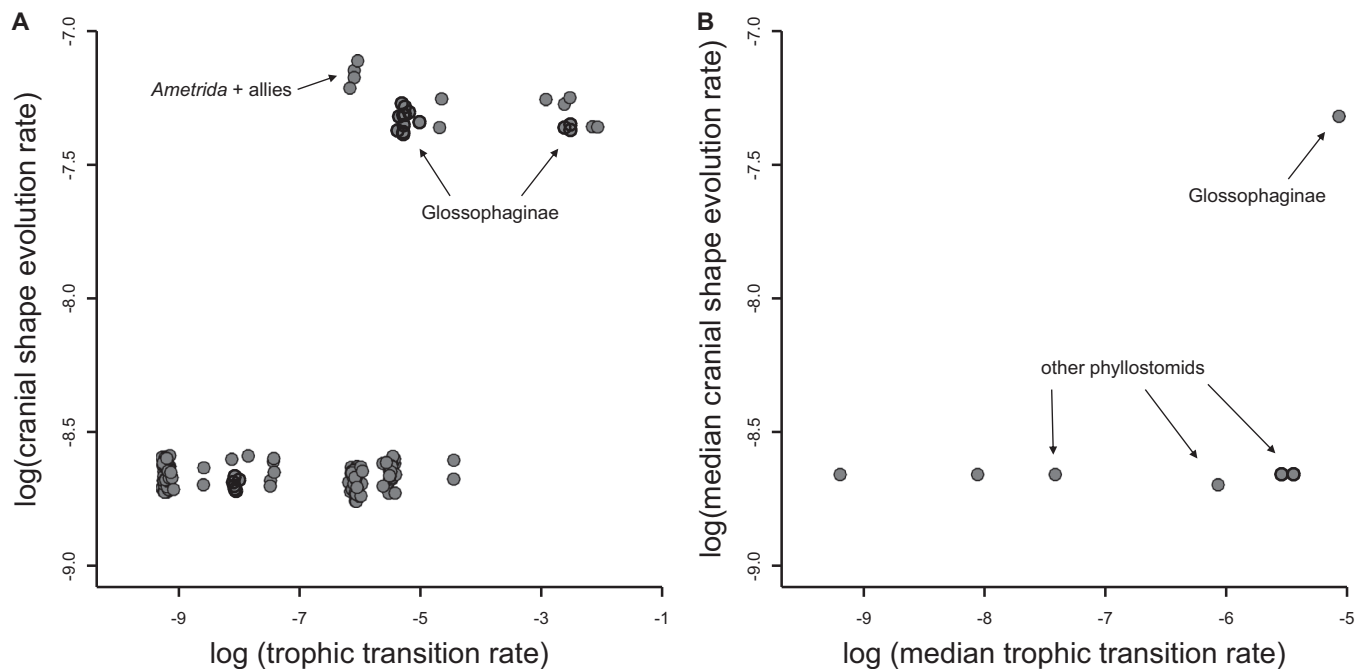
Figure 5. Trophic and morphological rates. (A) Species-level ecological transition rates and cranial shape evolution rates. An apparent linear relationship between the two is entirely driven by Glossophaginae, the only clade with high rates in both processes. *Ametria* + allies are the only other small clade with rapid shape evolution rates. (B) Median ecological transition rates and cranial shape evolution rates for trophic cohorts. Although phyllostomids vary overall in ecological dynamics, only glossophagines show rapid rates of both trophic niche and cranial evolution. In both subplots, points are jittered slightly for clarity.

21 glossophagine species with rapid rates of both trophic and cranial evolution (see Supporting Information for a permutation test of significance and associated discussion). One-third of glossophagines (*Glossophaga* and *Leptonycteris*) have absolute PGLS studentized residuals > 3, and median absolute residuals for this clade are more than twice that of all non-glossophagines, potentially indicating that glossophagines are significant outliers. If we remove this clade, the positive relationship essentially disappears (OLS $R^2 = 0.00192$). The coefficient of variation for morphological rates is much lower (0.74) than that of trophic rates (3.09).

Discussion

We tested for rate-coupling between two different evolutionary processes—cranial shape evolution and trophic evolution—during the radiation of New World bats. In addition, we present a model-averaging framework that can be used to quantify heterogeneity in rates of phenotypic evolution on phylogenetic trees. Overall, we find evidence for multiple trophic cohorts and considerable variation in rates of trophic evolution for this clade. Cranial shape evolution, by contrast, is characterized by relatively homogeneous rates and few well-supported cohorts. Furthermore, there is only a single clade (Fig. 1; Phyllostomidae: Glossophaginae) that has fast rates of both trophic and cranial

evolution (Fig. 5). Most other clades that evolve rapidly in trophic space are not characterized by relatively rapid rates of cranial shape evolution, compared to the rest of the radiation. There are several potential interpretations of these data and results. First, we consider the effects of underestimating plasticity in Neotropical bat trophic ecology. If many New World bat species are functionally versatile, then their trophic evolution may be governed by an underlying, more homogeneous process that is coupled with morphological lability. Alternatively, New World bats could represent one example of a macroevolutionary paradigm where trophic and morphological evolution are largely decoupled processes at this scale, despite established ecomorphological and functional associations in bat feeding ecology.

TROPHIC AND MORPHOLOGICAL DYNAMICS

We find evidence for heterogeneous dynamics of trophic evolution, especially within the superfamily Noctilionoidea and its largest family Phyllostomidae (Fig. 1). The nectarivorous and omnivorous subfamily Glossophaginae is characterized by the fastest transition rates among guilds (Figs. 2 and 5), as is the trophically diverse, paraphyletic complex (Hoffmann et al. 2008) comprising Lonchophyllinae and many other phyllostomids (Table 1). By contrast, stenodermatines are characterized by relatively slow rates of trophic evolution (Fig. 2B)—perhaps notably so, considering their rapid speciation rates (Shi and

Rabosky 2015; Rojas et al. 2016). Their ability to process hard fruits is often described as a key innovation (Dumont et al. 2012) that precipitated rapid speciation. Insectivores are characterized by the slowest rates of trophic evolution (Fig. 2; Table 1). This is unsurprising, as such a static trophic state spanning much of the phylogeny likely reflects a slowly evolving process. Slow rates also characterize the obligately sanguivorous vampire bats (Table S1).

By contrast, dynamics of cranial shape evolution across New World bats are relatively homogeneous, even with the disparity present within guilds (Fig. 3). Importantly, this finding means that rates are relatively comparable across the radiation, but does not imply that rates of cranial evolution are generally slow or static. Most species are united into a single, paraphyletic morphological cohort (Table 1; Fig. 4A), and cranial disparity is better predicted by clade age than by trophic ecology (Fig. S4; Table S2). We only find significantly elevated rates of shape evolution for two groups: glossophagines and a clade of four of the most morphologically unique stenodermatine genera (*Ametrida*, *Centurio*, *Pygoderma*, and *Sphaeronycteris*). This small clade of *Ametrida* and allies stands out from the rest of stenodermatines for its rapid morphological evolution despite apparent trophic stasis.

Glossophagines are the only cohort identified with relatively elevated rates of evolution for *both* trophic ecology and morphology (Fig. 5). This is perhaps unsurprising, given that these bats both have particularly divergent snout morphologies and readily shift from nectar to fruit across species (Fig. 1; Table S1). Outside of glossophagines, however, the overall pattern appears to be that New World bats are generally homogeneous in dynamics of cranial shape evolution, yet heterogeneous in dynamics of trophic evolution.

TROPHIC ECOLOGY AND CLASSIFICATION: AN OMNIVORES' DILEMMA?

Why does trophic evolution appear largely decoupled from cranial shape evolution in these bats (Fig. 5)? One possibility is that many species are far more generalized and behaviorally plastic in their trophic ecology than is often assumed—this may especially be the case with noctilionoids, which comprise most of New World bat diversity (Fig. 1). Even the most morphologically specialized noctilionoid nectarivores regularly supplement their diets with insects and fruits, and vice versa, despite predicted biomechanical trade-offs (Winter and von Helversen 2003; Barros et al. 2013). Phyllostomid diets are now known to be more general than is historically assumed, even across foods of very different material properties (Rex et al. 2010; Oelbaum et al. 2019), and in spite of overall skull shape generally predicting performance (Figure 3; Santana et al. 2010, Santana et al. 2012). Even within insectivores (Bell 1982; Lenhart et al. 2010) and vampires (Carter et al. 2006;

Voigt and Kelm 2006) throughout the radiation, variable and potentially opportunistic hunting behaviors are masked by simple classifications of "specialist" insectivory or sanguivory.

Furthermore, in this radiation, it seems likely that the most common transitions are between specialist and generalist (e.g., omnivory) states, as opposed to among the specialist states (Fig. 1). It is possible that trophic state evolution in this direction, and at this time scale, occurs without obvious signals of accompanying cranial divergence. In other words, because specialized cranial shapes can also perform adequately for more generalist behavior, we may not expect to see the large-scale morphological shifts associated with transitions among highly divergent specialist behaviors. Transitions among specialist states, such as insectivory or frugivory, may occur at much deeper timescales, and with clear separation among their associated morphospaces (Fig. 3).

Generalist behavior and resource switching despite apparent morphological specialization, or "functional versatility," potentially explains high species richness in other radiations (Robinson and Wilson 1998; Bellwood et al. 2006). For example, species that typically appear and function as specialists could opportunistically switch diets across the resource spectrum when competition is high, potentially facilitating higher levels of diversity. If many more species could be and were classified as omnivores, then we might expect to infer more homogeneous dynamics of trophic evolution, reconciling them with morphological dynamics. Although omnivory may be a macroevolutionary dead-end in other major vertebrate clades (Burin et al. 2016), this appears to be highly unlikely with noctilionoids (Rojas et al. 2018).

Unfortunately, thresholds for classifying a species as one discrete state over another are unavoidably arbitrary at some level, and are highly sensitive to sampling and observation, or seasonal and temporal variation. Yet the degree to which many noctilionoids can be considered omnivorous or otherwise ecologically flexible could have major repercussions for interpreting macroevolutionary dynamics of the New World bat radiation. Consider, for example, the possibility that trophic rates are particularly rapid along terminal branches of the phylogeny, leading to ephemeral or multivariate trophic states at shallow, ecological timescales. These trophic shifts are potentially associated with modular and/or granular shifts in cranial morphology, perhaps not detectable at the scale of our data here. Newly developed methods could allow researchers to model complex (multivariate) ecological phenotypes on phylogenies with these hypotheses in mind (Grundler and Rabosky 2020a). Further development of a quantitative and comprehensive database of proportional resource use across bats would enable researchers to minimize errors due to arbitrary and oversimplifying state classification.

ECOMORPHOLOGY WITHIN EVOLUTIONARY RADIATIONS

By contrast, consider if these character states are a valid approximation of realized trophic ecology in bats. This implies a decoupling of trophic and morphological dynamics, and niche differentiation without accompanying strong morphological divergence. Our findings would thus be analogous to those of Blankers et al. (2012), who also found uncorrelated ecological and morphological dynamics in another vertebrate system. The general and homogeneous morphological process shared across most of the phylogeny (Fig. 4) could be interpreted as one of relative cranial lability, with high overall rates that allow for the observed accumulation of intra-guild disparity (Fig. 3). In other words, bat cranial morphology could be characterized by high evolutionary rates across the radiation, despite little rate variation between the subclades. Mammalian crania in general may exhibit this high lability over macroevolutionary timescales, especially in comparison with soft tissue, mandibles, or teeth (Linde-Medina et al. 2016). Furthermore, generally high cranial lability, even in the absence of rate variation, does not preclude granular morphological specializations and adaptations to specific diet items. These morphological specializations could occur at a scale too fine to infer here, but may exhibit more tight coupling with trophic evolution.

This dataset broadly captures overall cranial shape, but individual crania do not always function as integrated units that uniformly serve the same ecomorphological functions. Our findings must thus also be interpreted within the context of skull modularity. Bat crania, like those of other mammals, can be highly modular and linked to other aspects of behavior or sensory ecology (Goswami 2006; Machado et al. 2007; Curtis and Simmons 2017). The mandible and its associated muscles, on the other hand, are more integrated and functionally constrained (Santana et al. 2010; López-Aguirre et al. 2015). It is possible that these cranial shape characters are an overall weak proxy for ecological function (Feilich and López-Fernández 2019), though prior ecomorphological research on bat skulls and crania suggests this is unlikely at a broad phylogenetic scale (Dumont et al. 2012; Santana et al. 2012; Santana and Cheung 2016).

We nonetheless acknowledge the possibility that these results are driven by evolutionary divergence along morphological axes that are not fundamental to trophic performance. It does appear that mandibular shape evolution is more tightly coupled with trophic evolution (Arbour et al. 2019), and could disproportionately drive the well-established ecomorphological relationships between overall skull shape and trophic states in New World bats. We may expect to find a closer coupling between mandibular shape and trophic evolution, or even between finer-scaled cranial modules and trophic evolution. On the other hand, mandibles are also functionally linked with the cranium, and it is thus also possible that we would find an analogously decoupled relationship between mandibular and trophic evolution. At the broadest scale, homogeneous and labile dynamics of morphological evolution could be one indicator that bat diversity is unsaturated at macroevolutionary scales (sensu Harmon and Harrison 2015), and/or expanding (Shi and Rabosky 2015), thus providing a potential counterexample to the strong diversity dependence that characterizes some other radiations (Rabosky 2009).

Positive correlations between morphological evolution and lineage diversification are often considered to be hallmarks of adaptive radiation, as rapid trait evolution and diversification are further often associated with and reinforced by ecological divergence (Schluter 2000; Losos and Mahler 2010). In these New World bats, however, the relationship between morphological and trophic evolution is less clear. Furthermore, they have rapidly speciated under a relatively homogeneous diversification regime (Shi and Rabosky 2015). We suggest that if we can clearly resolve omnivory in noctilionoids, New World bats could represent one example of decoupled processes that are frequently linked within adaptive radiations (Schluter 2000). Perhaps more surprisingly, the ecological diversity of these bats has clearly flourished despite relatively homogeneous dynamics of speciation and shape evolution, suggesting that hyperdiverse clades can emerge even in the absence of coupling between rates of ecological and phenotypic change.

DATA ARCHIVING

All new data and code supporting the results and for performing the analyses are archived and available on Dryad (https://doi.org/10.5061/dryad.ghx3ffbn3).

CONFLICT OF INTEREST

The authors declare no conflict of interest.

LITERATURE CITED

Adams, D. C. 2014a. A generalized K statistic for estimating phylogenetic signal from shape and other high-dimensional multivariate data. Syst. Biol. 63:685–697.

———. 2014b. A method for assessing phylogenetic least squares models for shape and other high-dimensional multivariate data. Evolution 68:2675–2688.

———. 2014c. Quantifying and comparing phylogenetic evolutionary rates for shape and other high-dimensional phenotypic data. Syst. Biol. 63:166–177.

Adams, D. C., and M. L. Collyer. 2018. Multivariate phylogenetic comparative methods: evaluations, comparisons, and recommendations. Syst. Biol. 67:14–31.

———. 2015. Permutation tests for phylogenetic comparative analyses of high-dimensional shape data: what you shuffle matters. Evolution 69:823–829.

Adams, D. C., M. L. Collyer, A. Kaliontzopoulou, and E. Sherratt. 2017. Geomorph: software for geometric morphometric analyses. Version 3.0.6.

Arbour, J. H., A. A. Curtis, and S. E. Santana. 2019. Signatures of echolocation and dietary ecology in the adaptive radiation of skull shape in bats. Nat. Comm. 10:2036.

Arnold, S. J. 1983. Morphology, performance, and fitness. Am. Zool. 23:347–361.

Barros, M. A. S., A. M. Rui, and M. E. Fabian. 2013. Seasonal variation in the diet of the bat *Anoura caudifer* (Phyllostomidae: Glossophaginae) at the southern limit of its geographic range. Acta Chiropterol. 15:77–84.

Bell, G. P. 1982. Behavioral and ecological aspects of gleaning by a desert insectivorous bat *Antrozous pallidus* (Chiroptera: Vespertilionidae). Behav. Ecol. Sociobiol. 10:217–223.

Bellwood, D. R., P. C. Wainwright, C. J. Fulton, and A. S. Hoey. 2006. Functional versatility supports coral reef biodiversity. Proc. R. Soc. Lond. B Biol. Sci. 273:101–107.

Berwaerts, K., H. Van Dyck, and P. Aerts. 2002. Does flight morphology relate to flight performance? An experimental test with the butterfly *Pararge aegeria*. Funct. Ecol. 16:484–491.

Blankers, T., D. C. Adams, and J. J. Wiens. 2012. Ecological radiation with limited morphological diversification in salamanders. J. Evol. Biol. 25:634–646.

Blomberg, S. P., T. Garland, Jr., and A. R. Ives. 2003. Testing for phylogenetic signal in comparative data: behavioral traits are more labile. Evolution 57:717–745.

Burin, G., W. D. Kissling, P. R. Guimarães, Ç. H. Şekercioğlu, and T. B. Quental. 2016. Omnivory in birds is a macroevolutionary sink. Nat. Comm. 7:11250.

Calsbeek, R., and D. J. Irschick. 2007. The quick and the dead: correlational selection on morphology, performance, and habitat use in island lizards. Evolution 61:2493–2503.

Carter, G. G., C. E. Coen, L. M. Stenzler, and I. J. Lovette. 2006. Avian host DNA isolated from the feces of white-winged vampire bats (*Diaemus youngi*). Acta Chiropterol. 8:255–258.

Clavel, J., and H. Morlon. 2020. Reliable phylogenetic regressions for multivariate comparative data: illustration with the MANOVA and application to the effect of diet on mandible morphology in phyllostomid bats. Syst. Biol. 69:927–943.

Clavel, J., G. Escarguel, and G. Merceron. 2015. mvMORPH: an R package for fitting multivariate evolutionary models to morphometric data. Methods Ecol. Evol. 6:1311–1319.

Cooney, C. R., and G. H. Thomas. 2020. Heterogeneous relationships between rates of speciation and body size evolution across vertebrate clades. Nat. Ecol. Evol. 5:101–110.

Cozzolino, S., and A. Widmer. 2005. Orchid diversity: an evolutionary consequence of deception? Trends Ecol. Evol. 20:487–494.

Curtis, A. A., and N. B. Simmons. 2017. Unique turbinal morphology in horseshoe bats (Chiroptera: Rhinolophidae). Anat. Rec. 300:309–325.

Davis Rabosky, A. R., C. L. Cox, D. L. Rabosky, P. O. Title, I. A. Holmes, A. Feldman, and J. A. McGuire. 2016. Coral snakes predict the evolution of mimicry across New World snakes. Nat. Comm. 7:11484.

Dawideit, B. A., A. B. Phillimore, I. Laube, B. Leisler, and K. Böhning-Gaese. 2009. Ecomorphological predictors of natal dispersal distances in birds. J. Anim. Ecol. 78:388–395.

Denton, J. S. S., and D. C. Adams. 2015. A new phylogenetic test for comparing multiple high-dimensional evolutionary rates suggests interplay of evolutionary rates and modularity in lanternfishes (Myctophiformes; Myctophidae). Evolution 69:2425–2440.

Dumont, E. R., I. R. Grosse, and G. J. Slater. 2009. Requirements for comparing the performance of finite element models of biological structures. J. Theor. Biol. 256:96–103.

Dumont, E. R., L. M. Dávalos, A. Goldberg, S. E. Santana, K. Rex, and C. C. Voigt. 2012. Morphological innovation, diversification and invasion of a new adaptive zone. Proc. R. Soc. Lond. B Biol. Sci. 279:1797–1805.

Feilich, K. L., and H. López-Fernández. 2019. When does form reflect function? Acknowledging and supporting ecomorphological assumptions. Integr. Comp. Biol. 59:358–370.

FitzJohn, R. G. 2012. Diversitree: comparative phylogenetic analyses of diversification in R. Methods Ecol. Evol. 3:1084–1092.

Fleming, T., and W. Kress. 2013. The ornaments of life: coevolution and conservation in the tropics. Univ. of Chicago Press, Chicago.

Gillespie, R. 2004. Community assembly through adaptive radiation in Hawaiian spiders. Science 303:356–359.

Goswami, A. 2006. Cranial modularity shifts during mammalian evolution. Am. Nat. 168:270–280.

Gould, S. J., and N. Eldredge. 1993. Punctuated equilibrium comes of age. Nature 366:223–227.

Gunz, P., P. Mitteroecker, S. Neubauer, G. W. Weber, and F. L. Bookstein. 2009. Principles for the virtual reconstruction of hominin crania. J. Hum. Evol. 57:48–62.

Grundler, M. C., and D. L. Rabosky. 2020a. Complex ecological phenotypes on phylogenetic trees: a Markov process model for comparative analysis of multivariate count data. Syst. Biol. https://doi.org/10.1093/sysbio/syaa031.

———. 2020b. Macroevolutionary analysis of discrete traits with rate heterogeneity. BioRxivhttps://doi.org/10.1101/2020.01.07.897777.

Harmon, L. J., and H. Harrison. 2015. Species diversity is dynamic and unbounded at local and continental scales. Am. Nat. 185:584–593.

Hoffmann, F. G., S. R. Hoofer, and R. J. Baker. 2008. Molecular dating of the diversification of Phyllostominae bats based on nuclear and mitochondrial DNA sequences. Mol. Phylogenet. Evol. 49:653–658.

Jones, K. E., O. R. P. Bininda-Emonds, and J. L. Gittleman. 2005. Bats, clocks, and rocks: diversification patterns in Chiroptera. Evolution 59:2243–2255.

Kingsolver, J. G., and R. B. Huey. 2003. Introduction: the evolution of morphology, performance, and fitness. Integr. Comp. Biol. 43:361–366.

Klingenberg, C. P., and J. Marugán-Lobón. 2013. Evolutionary covariation in geometric morphometric data: analyzing integration, modularity, and allometry in a phylogenetic context. Syst. Biol. 62:591–610.

Kosnik, M. A., D. Jablonski, R. Lockwood, and P. M. Novack-Gottshall. 2006. Quantifying molluscan body size in evolutionary and ecological analyses: maximizing the return on data-collection efforts. Palaios 21:588–597.

Lenhart, P. A., V. Mata-Silva, and J. D. Johnson. 2010. Foods of the pallid bat, *Antrozous pallidus* (Chiroptera: Vespertilionidae), in the Chihuahuan desert of western Texas. Southwest. Nat. 55:110–115.

Linde-Medina, M., J. C. Boughner, S. E. Santana, and R. Diogo. 2016. Are more diverse parts of the mammalian skull more labile? Ecol. Evol. 6:2318–2324.

López-Aguirre, C., J. Pérez-Torres, and L. A. B. Wilson. 2015. Cranial and mandibular shape variation in the genus *Carollia* (Mammalia: Chiroptera) from Colombia: biogeographic patterns and morphological modularity. PeerJ 3:e1197.

Losos, J. B. 1990. The evolution of form and function: morphology and locomotor performance in West Indian *Anolis* lizards. Evolution 44:1189–1203.

Losos, J. B., and D. L. Mahler. 2010. Adaptive radiation: the interaction of ecological opportunity, adaptation, and speciation. Pp. 381–420 *in* M. Bell, D. Futuyma, W. Eanes, and J. Levinton, eds. Evolution since Darwin: The first 150 years. Sinauer Associates, Sunderland, MA.

Machado, M., E. M. dos Santos Schmidt, T. C. Margarido, and F. Montiani-Ferreira. 2007. A unique intraorbital osseous structure in the large fruit-eating bat (*Artibeus lituratus*). Vet. Ophthalmol. 10:100–105.

McGuire, J. L. 2010. Geometric morphometrics of vole (*Microtus californicus*) dentition as a new paleoclimate proxy: shape change along geographic and climatic clines. Quat. Int. 212:198–205.

Miles, D. B., and R. E. Ricklefs. 1984. The correlation between ecology and morphology in deciduous forest passerine birds. Ecology 65:1629–1640.

Monteiro, L. R., and M. R. Nogueira. 2011. Evolutionary patterns and processes in the radiation of phyllostomid bats. BMC Evol. Biol. 11:137.

Nowak, M. D. 1994. Walker's bats of the world. Johns Hopkins University Press, Baltimore, MD.

Oelbaum, P. J., M. B. Fenton, N. B. Simmons, and H. G. Broders. 2019. Community structure of a Neotropical bat fauna as revealed by stable isotope analysis: not all species fit neatly into predicted guilds. Biotropica 51:719–730.

Olson, D. M., E. Dinerstein, E. D. Wikramanayake, N. D. Burgess, G. V. N. Powell, E. C. Underwood, J. A. D'amico, I. Itoua, H. E. Strand, J. C. Morrison, et al. 2001. Terrestrial ecoregions of the world: a new map of life on Earth. BioScience 51:933–938.

Osborn, H. F. 1902. The law of adaptive radiation. Am. Nat. 36:353–363.

Rabosky, D. L. 2009. Ecological limits on clade diversification in higher taxa. Am. Nat. 173:662–674.

Rabosky, D. L., F. Santini, J. Eastman, S. A. Smith, B. Sidlauskas, J. Chang, and M. E. Alfaro. 2013. Rates of speciation and morphological evolution are correlated across the largest vertebrate radiation. Nat. Comm. 4:1958.

Rabosky, D. L., S. C. Donellan, M. C. Grundler, and I. J. Lovette. 2014a. Analysis and visualization of complex macroevolutionary dynamics: an example from Australian scincid lizards. Syst. Biol. 63:610–627.

Rabosky, D. L., M. C. Grundler, C. J. R. Anderson, P. O. Title, J. J. Shi, J. W. Brown, H. Huang, and J. G. Larson. 2014b. BAMMtools: an R package for the analysis of evolutionary dynamics on phylogenetic trees. Methods Ecol. Evol. 5:701–707.

Revell, L. J., and D. C. Collar. 2009. Phylogenetic of the evolutionary correlation using likelihood. Evolution 63:1090–1100.

Revell, L. J., and L. J. Harmon. 2008. Testing quantitative genetic hypotheses about the evolutionary rate matrix for continuous characters. Evol. Ecol. Res. 10:311–331.

Rex, K., B. I. Czaczkes, R. Michener, T. H. Kunz, and C. C. Voigt. 2010. Specialization and omnivory in diverse mammalian assemblages. Ecoscience 17:37–46.

Ricklefs, R. E. 2004. Cladogenesis and morphological diversification in passerine birds. Nature 430:338–341.

Robinson, B. W., and D. S. Wilson. 1998. Optimal foraging, specialization, and a solution to Liem's paradox. Am. Nat. 151:223–235.

Rohlf, F. J. 2010. tpsRelw: relative warps analysis. Version 1.49.

Rohlf, F. J., and D. Slice. 1990. Extensions of the Procrustes method for the optimal superimposition of landmarks. Syst. Zool. 39:40–59.

Rojas, D., O. M. Warsi, and L. M. Dávalos. 2016. Bats (Chiroptera: Noctilionoidea) challenge a recent origin of extant Neotropical diversity. Syst. Biol. 65:432–448.

Rojas, D., M. J. Ramos Pereira, C. Fonseca, and L. M. Dávalos. 2018. Eating down the food chain: generalism is not an evolutionary dead end for herbivores. Ecol. Lett. 21:402–410.

Rundell, R. J., and T. D. Price. 2009. Adaptive radiation, nonadaptive radiation, ecological speciation and nonecological speciation. Trends Ecol. Evol. 24:394–399.

Santana, S. E., and E. Cheung. 2016. Go big or go fish: morphological specializations in carnivorous bats. Proc. R. Soc. Lond. B Biol. Sci. 283:20160615.

Santana, S. E., and E. R. Dumont. 2009. Connecting behaviour and performance: the evolution of biting behaviour and bite performance in bats. J. Evol. Biol. 22:2131–2145.

Santana, S. E., and S. E. Lofgren. 2013. Does nasal echolocation influence the modularity of the mammal skull? J. Evol. Biol. 26:2520–2526.

Santana, S. E., E. R. Dumont, and J. L. Davis. 2010. Mechanics of bite force production and its relationship to diet in bats. Funct. Ecol. 24:776–784.

Santana, S. E., I. R. Grosse, and E. R. Dumont. 2012. Dietary hardness, loading behavior, and the evolution of skull form in bats. Evolution 66:2587–2598.

Schluter, D. 1996. Ecological causes of adaptive radiation. Am. Nat. 148:S40–S64.

———. 2000. The ecology of adaptive radiation. Oxford Univ. Press, Oxford, U.K.

Serb, J. M., E. Sherratt, A. Alejandrino, and D. C. Adams. 2017. Phylogenetic convergence and multiple shell shape optima for gliding scallops (Bivalvia: Pectinidae). J. Evol. Biol. 30:1736–1747.

Sherratt, E., D. J. Gower, C. P. Klingenberg, and M. Wilkinson. 2014. Evolution of cranial shape in caecilians (Amphibia: Gymnophiona). Evol. Biol. 41:528–545.

Shi, J. J., and D. L. Rabosky. 2015. Speciation dynamics during the global radiation of extant bats. Evolution 69:1528–1545.

Shi, J. J., E. P. Westeen, N. T. Katlein, E. R. Dumont, and D. L. Rabosky. 2018a. Ecomorphological and phylogenetic controls on sympatry across extant bats. J. Biogeog. 45:1560–1570.

Shi, J. J., E. P. Westeen, and D. L. Rabosky. 2018b. Digitizing extant bat diversity: an open-access repository of 3D, μCT-scanned skulls for research and education. PLoS ONE 13:e0203022.

Simmons, N. B. 2005. Order Chiroptera. Pp. 312–529 *in* D. E. Wilson and D. M. Reeder, eds. Mammal species of the world: a taxonomic and geographic reference. Johns Hopkins Univ. Press, Baltimore, MD.

Simmons, N. B., and T. M. Conway. 2003. Evolution of ecological diversity in bats. Pp. 493–535 *in* Bat ecology, ed. Univ. of Chicago Press, Chicago.

Simpson, G. G. 1953. The major features of evolution. Columbia City Press, New York.

Stebbins, G. L. 1970. Adaptive radiation of reproductive characteristics in angiosperms, I: pollination mechanisms. Annu. Rev. Ecol. Syst. 1:307–326.

Sturmbauer, C. 1998. Explosive speciation in cichlid fishes of the African Great Lakes: a dynamic model of adaptive radiation. J. Fish Biol. 53:18–36.

Teeling, E. C., M. S. Springer, O. Madsen, P. Bates, S. J. O'Brien, and W. J. Murphy. 2005. A molecular phylogeny for bats illuminates biogeography and the fossil record. Science 307:580–584.

Voigt, C. C., and D. H. Kelm. 2006. Host preference of the common vampire bat (*Desmodus rotundus*; Chiroptera) assessed by stable isotopes. J. Mammal. 87:1–6.

Wagner, C. E., L. J. Harmon, and O. Seehausen. 2012. Ecological opportunity and sexual selection together predict adaptive radiation. Nature 487:366–369.

Winter, Y., and O. von Helversen. 2003. Operational tongue length in phyllostomid nectar-feeding bats. J. Mammal. 84:886–896.

Yang, A. S. 2001. Modularity, evolvability, and adaptive radiations: a comparison of the hemi-and holometabolous insects. Evol. Dev. 3:59–72.

Zanno, L. E., and P. J. Makovicky. 2011. Herbivorous ecomorphology and specialization patterns in theropod dinosaur evolution. Proc. Natl. Acad. Sci. USA 108:232–237.

Zelditch, M. L., J. Ye, J. S. Mitchell, and D. L. Swiderski. 2017. Rare ecomorphological convergence on a complex adaptive landscape: body size and diet mediate evolution of jaw shape in squirrels (Sciuridae). Evolution 71:633–649.

Supporting Information

Additional supporting information may be found online in the Supporting Information section at the end of the article.

Supplementary Material

Table S1. (Separate file due to size) A summary of all metadata associated with the 167 cranial specimens used for this study.

Table S2. We calculated and assessed the significance of differences in Procrustes variances (disparity) as predicted by three potential covariates: families, ecological guilds, and our ecological cohorts.

Table S3. Constrained three-rate BMM model fits, in *mvMORPH*, to PC axes 1-3 of our cranial shape data, ranked by Akaike weight.

Table S4. *Convergence in cranial shape - a distance-based criterion*.

Table S5. In addition to testing for convergence within ecological guilds, we also specifically tested for convergence between vampire bat crania and each of the major trophic categories within noctilionoids (insectivores, nectarivores, omnivores).

Figure S1. An illustration of our cohort-based approach for this study, using a phylogeny with three clades *A*, *B*, and *C*. Species *within* each clade have 100% pairwise probability of belonging to the same cohort as each, across all potential models (after factoring in their respective Akaike weight).

Figure S2. Landmarking scheme used for digitizing shape data, on a specimen of *Artibeus aztecus* (Noctilionoidea: Phyllostomidae: Stenodermatinae).

Figure S3. On the left, a plot of cumulative Akaike weights over all split-Mk models of trophic evolution, analogous to a scree plot for factor analyses.

Figure S4. A simple hypothesis for how and why shape varies across phylogenies would be that higher clade disparity is best predicted by older clade age.

Figure S5. After discarding all potential BMM morphological models (R-mode) that had partitions with < 4 species (given our three axes), we fitted a total of 3,829 one-, two-, and three-rate models to the data.

Figure S6. The species-level phylogeny of New World bats included in this study, and associated variation across the first three principal component (PC) axes.

Figure S7. *Results from analyses with multiple trophic states per taxon*.

Figure S8. A modified version of Figure 1 from the main text, with alternative trophic ecology labels.

Figure S9. A modified version of Figure 3 in the main text, including convex hulls for large trophic cohorts and some alternative crania.